Supporting Information

pH-Responsive Smart Hydrogel Dressing for Controlled Antimicrobial Therapy and Accelerated Wound Healing

Essam A.M.S. Obaid, Ruining Bai, and Zhifeng Fu *

Key Laboratory of Luminescence Analysis and Molecular Sensing (Ministry of Education), College of Pharmaceutical Sciences, Southwest University, Chongqing 400715, China

* E-mail address: fuzf@swu.edu.cn

Materials

AM and TEMED were purchased from Shanghai Macklin Biochemical Co., Ltd. (China). BIS was purchased from Shanghai Titan Scientific Co., Ltd. (China). APS was purchased from Chengdu Kelong Chemical Co., Ltd. (China). $AgNO_3$ was obtained from Chron Chemical Co., Ltd. (China). HA (5 kD) was obtained from Freda Biochem Co., Ltd. (China). Hyaluronidase (HAase) and apigenin stock solution (10 mM, 1 mL in DMSO) were purchased from MedChemExpress (MCE). Luria-Bertani (LB) agar was purchased from Oxoid Ltd (UK). Live/dead bacteria kit was acquired from Avtech Huailai Co., Ltd. (China). FBS, RPMI 1640 medium, and Dulbecco's Modified Eagle Medium (DMEM, high glucose) were obtained from Biological Industries (China). Deuterated solvents including deuterated dimethyl sulfoxide (DMSO-d6) and deuterated methanol (methanol-d4) were purchased from Sun Chemical Technology Co., Ltd. (China). CellTiter 96™ AQueous One Solution Cell Proliferation Assay (MTS) kit was obtained from Thermo Fisher Scientific (USA).

Instruments

A JEM-2100EX transmission electron microscope (JEOL, Japan) and an SU8020 scanning electron microscope (Hitachi, Japan) were employed to obtain TEM and SEM images. FT-IR spectra were acquired using a Nicolet IS10 spectrophotometer (Thermo Scientific, USA). TGA was performed on a TA Q200 analyzer, with samples heated from 30°C to 800°C at a rate of 10°C/min under an argon atmosphere. XRD patterns were recorded using a Rigaku Ultima IV diffractometer equipped with a Cu-Kα radiation source, scanning over a 2θ range of 5°–50° at a rate of 6°/min. UV–Vis absorbance measurements were obtained using an Infinite M200 PRO microplate reader (TECAN Group Ltd., Switzerland). The pore size of the hydrogels was determined by measuring the pores from SEM images using ImageJ software.

pH-Responsive Evaluation of CV-Loaded Hydrogel

The in-vitro release behavior of the formulated hydrogel was evaluated in PBS with varying pH levels (4.0, 5.5,6.5 7.4, and 10.0) using a small, water-soluble fluorescent dye as the model

compound. The PAM/CV hydrogel was prepared using a CV solution, adopting a synthesis approach analogous to that employed for the PAM/Ag hydrogel. To remove any loosely adsorbed dye from the surface, the hydrogels were thoroughly rinsed prior to immersion in 10 mL of PBS at the designated pH values. The samples were incubated at 37 ± 0.5 °C in a shaking incubator set to 120 rpm to simulate physiological conditions. At predetermined time points (0.5, 1, 2, 4, 6, 8, 10, 12, 14, 18, 22 and 24 h), 1 mL aliquots were collected and immediately replaced with an equal volume of fresh buffer to maintain sink conditions. The release of the dye was quantified by measuring fluorescence intensity at excitation/emission wavelengths of 540/595 nm using a microplate reader, and the cumulative release was determined based on a standard calibration curve.

pH-Responsive PAM/Ag@HA Smart Hydrogel Swelling

The swelling behavior of the hydrogel across various pH environments was determined using a gravimetric technique, in accordance with previously reported methodologies.[1] Dried hydrogel samples, each weighing approximately 0.3 g, were immersed in PBS adjusted to pH values of 4.0, 5.5, 6.5, 7.4, and 10.0, reflecting physiological conditions relevant to both healthy skin and infected wound environments. The hydrogels were allowed to swell until equilibrium was achieved. At predetermined time intervals, samples were removed from the PBS, gently blotted with filter paper to eliminate excess surface moisture, and immediately weighed to assess their swelling capacity. The swelling percentage (SP) of the hydrogel was calculated using the following equation:

$$\text{Swelling}\ (\%) = \frac{W_S - W_d}{W_d} \times 100\% \qquad (1)$$

Where "W_s" is a weight of swollen gel and "W_d" is the weight of dry hydrogel.

Silver Ion Release from PAM/Ag@HA Smart Hydrogel in the presence of HAase

PAM/Ag@HA hydrogel (300 mg) was accurately weighed and immersed in 15 mL (pH 7.4) containing HAase (100 U mL^{-1}), without HAase, or with apigenin (HAase inhibitor) as the release media. The mixtures were incubated at 37 °C under continuous shaking at approximately 100 rpm. At predetermined time intervals (1, 6, 24, 48, and 72 h), 1 mL aliquots were withdrawn and replaced with an equal volume of fresh medium to maintain constant volume and sink conditions. The collected samples were centrifuged, and the concentration of released Ag^+ ions in the supernatant was quantified by ICP-MS.

Hemolysis of PAM/Ag and PAM/Ag@HA Smart Hydrogels

The hemolysis ratio was employed to assess the blood compatibility of the hydrogel materials, serving as an indicator of their potential to induce red blood cell lysis.[2] Briefly, 1 mL of freshly collected mouse blood was diluted with 1.25 mL of 0.9% (w/v) saline solution. Hydrogel samples were prepared in three different dimensions (5 mm, 30 mg; 8 mm, 50 mg; and 10 mm, 80 mg), thoroughly rinsed three times with 0.9% saline, and then incubated in 10 mL of saline suspension at 37 °C for 2 h to equilibrate. The corresponding concentrations were 3, 5, and 8 mg mL^{-1}, respectively. Subsequently, 0.2 mL of the diluted blood was added to each sample, followed by a further 1-h incubation at 37 °C. After incubation, the mixtures were centrifuged at 1500 rpm for 10 min. The absorbance of the supernatant was then measured at 545 nm to determine the extent of hemolysis. PBS and ultrapure water were used as the negative and positive controls, respectively. The hemolysis percentage was calculated using the following formula:

$$\text{Hemolysis ratio}\ (\%) = \frac{\text{OD sample} - \text{OD negative}}{\text{OD positive} - \text{OD negative}} \times 100\% \quad (2)$$

Where OD_{Sample}, $OD_{Negative}$, and $OD_{Positive}$ indicate the average absorbance values for the tested sample, the negative control, and the positive control, respectively.

In Vitro Cytotoxicity Assay

The in-vitro biocompatibility of PAM, PAM/Ag, and PAM/Ag@HA hydrogels was evaluated using Caco-2 and L-929 cell lines. Hydrogel specimens of varying sizes (5 mm, 30 mg; 8 mm, 50 mg; and 10 mm, 80 mg) were immersed in 10 mL of complete culture medium (DMEM, high glucose) supplemented with 10% FBS and incubated for 12 h to prepare the hydrogel extracts. The resulting supernatants were collected and used as test media for cytocompatibility analysis. The corresponding concentrations were 3, 5, and 8 mg mL^{-1}, respectively. Cells were exposed to these extracts for an additional 24 h, after which the MTT assay was employed to assess cell viability. Absorbance at 490 nm (OD490) was measured to quantify metabolic activity and evaluate any cytotoxic effects. Cell viability was calculated using the following formula:

$$\text{Cell viability}\ (\%) = \frac{\text{OD treatment groups}}{\text{OD control groups}} \times 100\% \quad (3)$$

Stability Study of PAM/Ag@HA Smart Hydrogel

To evaluate the stability of the PAM/Ag@HA hydrogel, TGA was conducted on 10 mm (80 mg) hydrogel samples from each formulation group to assess their thermal decomposition profiles. Additionally, identically sized hydrogel specimens were incubated for 24 h in three different media: ultrapure water, PBS, pH 7.4, and 10% FBS. Furthermore, ICP-MS was employed to determine the concentration of silver ions released into the surrounding media, offering insight into the release kinetics and environmental stability of the hydrogel under physiologically relevant conditions.

Bacterial Morphology Observation

SEM was employed to observe morphological alterations in bacterial cells following treatment with the prepared hydrogels.[3] Bacterial suspensions at a concentration of 10^{10} CFU mL^{-1} were exposed to the hydrogel samples for 6 h. Post-treatment, the bacterial cells were

harvested by centrifugation and washed thoroughly with PBS to remove residual materials. The samples were then fixed with 2.5% (w/v) glutaraldehyde and subjected to a graded ethanol dehydration series (30%, 50%, 70%, 80%, 90%, 95%, and 100%), with each step lasting 10 min. After dehydration, the specimens were air-dried and coated with a thin layer of gold using an ion sputter coater to enhance conductivity. Finally, the bacterial morphology was examined and imaged to assess structural damage induced by the hydrogels.

Live/Dead Staining of Bacteria

Following exposure to antimicrobial treatment, bacterial samples from each experimental group were subjected to viability analysis through dual staining with SYTO9 and PI. The staining process was conducted over a 30-min incubation period in the dark to ensure optimal dye penetration. Subsequently, samples were rinsed thoroughly with 0.9% NaCl solution three times to eliminate any unbound fluorophores. The distribution of viable (green fluorescence) and non-viable (red fluorescence) cells was then visualized and documented using a laser scanning confocal microscope. The proportion of live and dead cells was quantified using ImageJ software.

Assessment of Cell Migration via Scratch Assay

L-929 cells were seeded in 6-well plates at a density of 5×10^4 cells/well and incubated for 24 h. A linear scratch was made using a sterile 200-μL pipette tip, and the debris was removed with PBS. Two hundred microliters of complete medium containing 5 mg mL^{-1} hydrogels was then added, and the plates were incubated at 37 °C in a humidified atmosphere with 5% CO_2. Cell migration into the scratch area was observed at 0 and 24 h using phase-contrast microscopy. The wound area was analyzed with ImageJ software, and the migration rate was calculated accordingly.

$$\text{Cell migration rate } (\%) = \frac{A_{t0} - A_t}{A_{t0}} \times 100\% \quad (4)$$

Where A_{t0} is the scratch area at the initial time, and A_t is the scratch area at different subsequent time points.

Zone of Inhibition Assay

Overnight cultures of *E. coli*, *S. aureus*, and MRSA were prepared and subsequently diluted to a final bacterial concentration of 1×10^6 CFU mL^{-1}. Following this, 100 μL aliquots of each bacterial suspension were evenly spread onto the surface of freshly prepared agar plates. 5 mm (30 mg) discs of circular hydrogel were precisely punched from each test samples of PAM, PAM/Ag, and PAM/Ag@HA using a sterile biopsy punch. The discs were subjected to UV irradiation for 1 h to ensure sterilization prior to use. The treated agar plates were then incubated at 37 °C for 20 h. Post-incubation, antibacterial efficacy was assessed by measuring the diameter of the inhibition zones (mm) surrounding each hydrogel disc. The zone of inhibition was determined using ImageJ software.

Bacteria Culture

All bacterial strains were obtained from the China General Microbiological Culture Collection Center. The selected models included two Gram-positive *S. aureus* (ATCC 29213) and MRSA (ATCC 43300) alongside a Gram-negative *E. coli* O157:H7 (CICC 21530). All bacterial species were initially cultivated in LB medium. To prepare working cultures, isolated colonies from LB agar plates were aseptically inoculated into liquid LB broth and incubated overnight at 37 °C under aerobic conditions. Bacterial suspensions were then sub-cultured to reach the logarithmic growth phase, after which they were adjusted to a final concentration of 1×10^6 CFU mL^{-1} in fresh LB medium for subsequent experiments.

Animals

All experimental procedures were conducted in strict accordance with the Chinese Guidelines for the Care and Use of Laboratory Animals. Ethical approval for the study was granted by the Animal Experimental Ethics Committee of Southwest University (Ethics No. SWU_LAC2024040001). Male Kunming (KM) mice, aged seven weeks and weighing between

30 and 40 g, were sourced from Southwest University, China, and were utilized for the experiments described in this study.

Table S1. Comparison of PAM/Ag@HA hydrogel with representative pH-responsive silver-based wound dressings.

Reference	Base composition	Silver type	pH mechanism	Healing performance	Biosafety	Key advantages
This work	Hyaluronic acid + Acrylamide	AgNPs	Alkaline-triggered (pH 7.4–10)	14 days	High cytocompatibility; reduced Ag toxicity via controlled release	Physiologically relevant pH response; controlled Ag release; strong in vivo efficacy; promotes M2 macrophage polarization and tissue regeneration
4	Cationic guar gum	Silver nanozymes	Acidic-triggered (pH 5.6–6.4)	10 days	Good biocompatibility	Combined photothermal and antibacterial activity
5	Methylcellulose	AgNPs	Alkaline-triggered (pH ~12)	Not reported	Not reported	On-demand release strategy
6	Methacrylic acid + Acrylamide	AgNPs	Alkaline-triggered (pH 7.4–10)	Not reported	Biocompatible	On-demand AgNPs release triggered by pathogenic bacteria
7	N-isopropylacrylamide + Acrylic Acid	AgNPs	Swelling-triggered release	9 days.	Good biocompatibility	On-demand antimicrobial delivery specifically tailored to the chemical biomarkers of infection (alkaline pH).
8	Hydrazide Hyaluronic Acid + Silk Microfibers	AgNPs	Gel-sol transition	10 days	Good cytocompatibility	Painless dressing changes via pH-triggered removal and synergistic photothermal antibacterial effect.

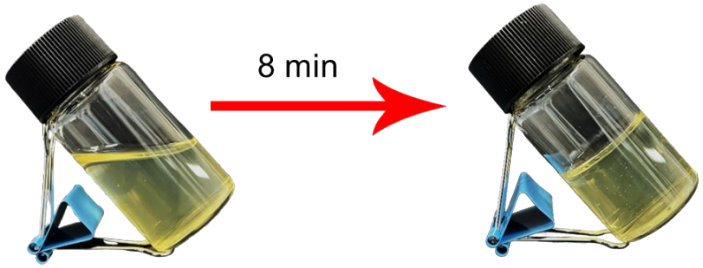

Fig. S1 Formation of PAM/Ag@HA hydrogel within 8 min after adding TEMED.

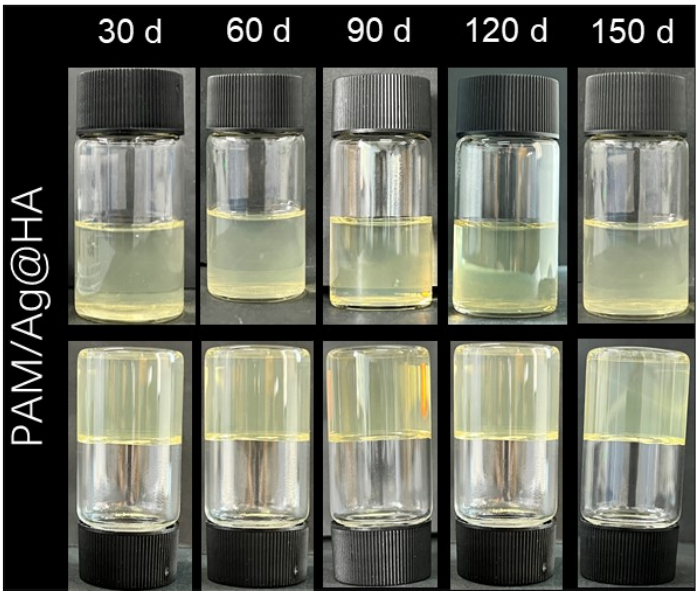

Fig. S2 Physical appearance of PAM/Ag@HA hydrogel after 150 days of storage at room temperature.

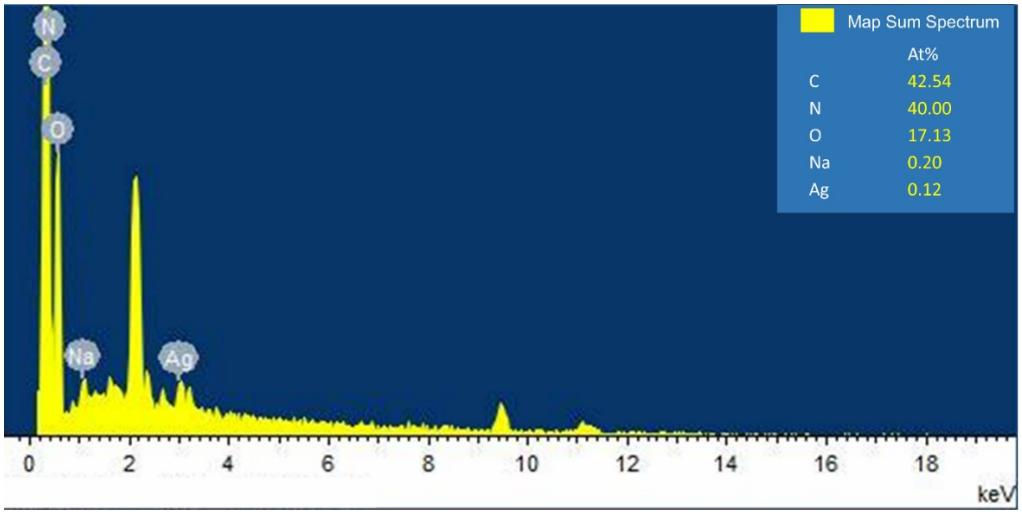

Fig. S3 EDX analysis of PAM/Ag@HA hydrogel.

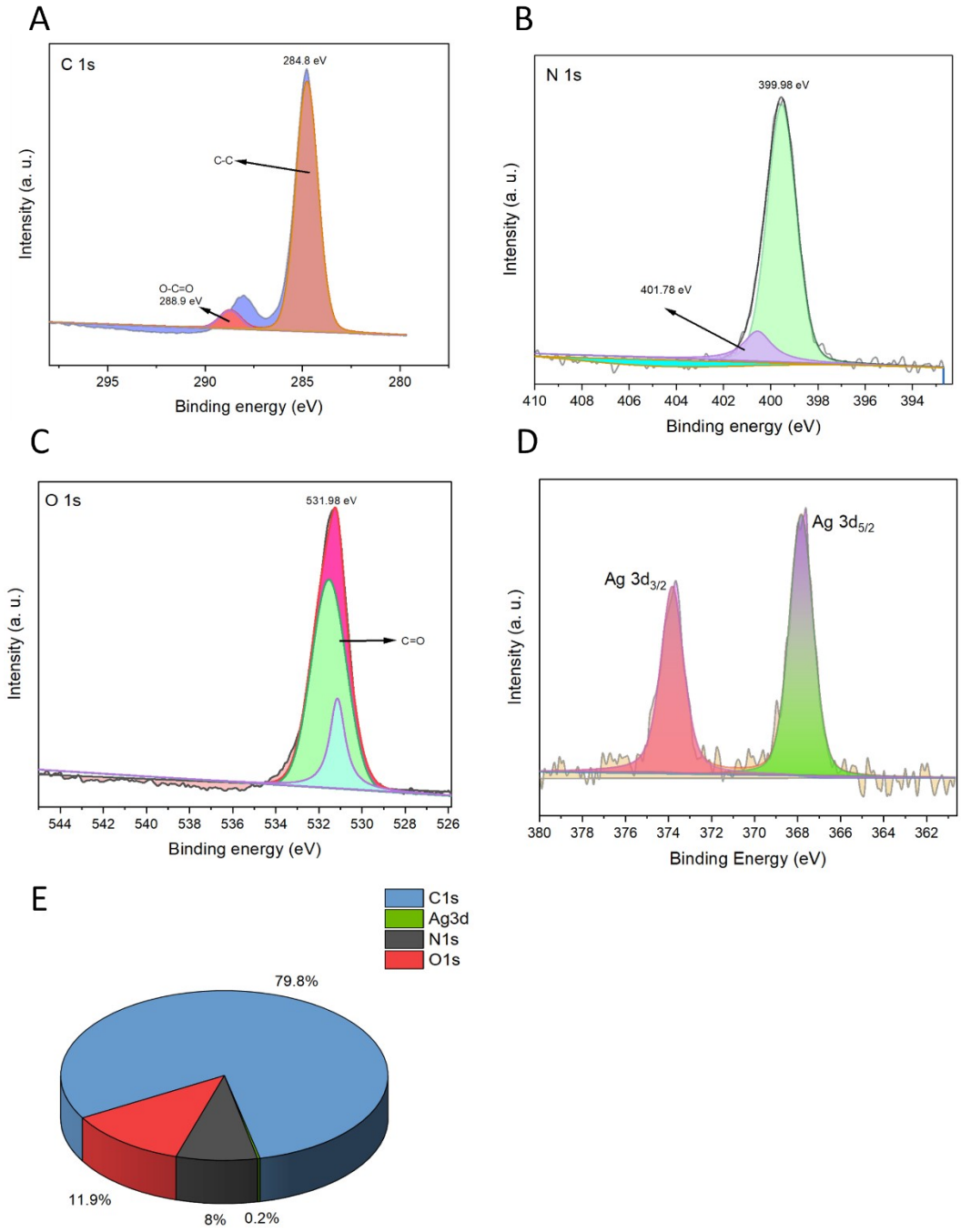

Fig. S4 High-resolution XPS spectra of (A) C 1s, (B) N 1s, and (C) O 1s. (D) Ag 3d binding energy spectra of PAM/Ag@HA hydrogel. (E) Elemental composition expressed as atomic percentages in PAM/Ag@HA hydrogel.

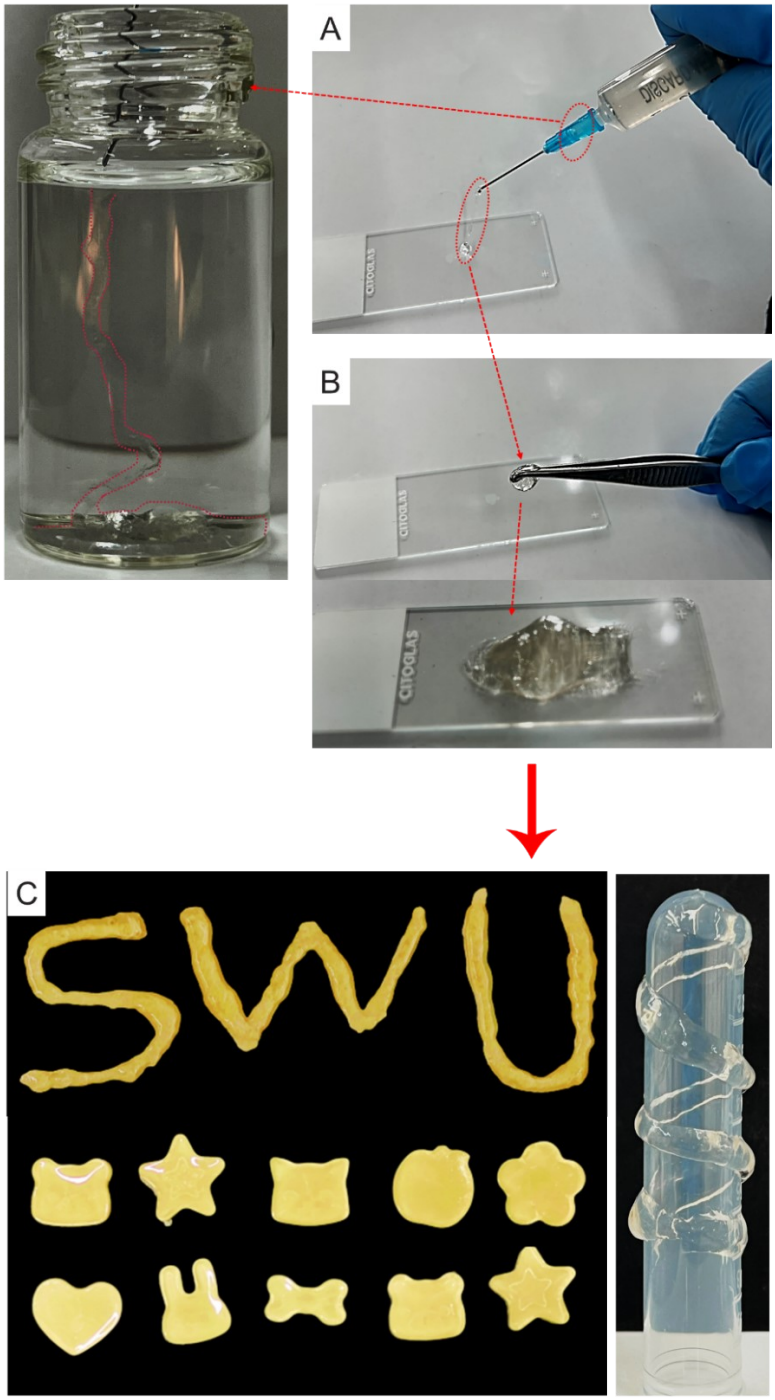

Fig. S5 The injectable performance of PAM/Ag@HA hydrogel: (A) The hydrogel was loaded into a syringe equipped with a 23-gauge needle and extruded smoothly without clogging. (B) The broken hydrogel fragments rapidly reformed into an integrated structure at room temperature without any external stimuli. (C) PAM/Ag@HA adhesive self-healing hydrogel could be molded into various shapes.

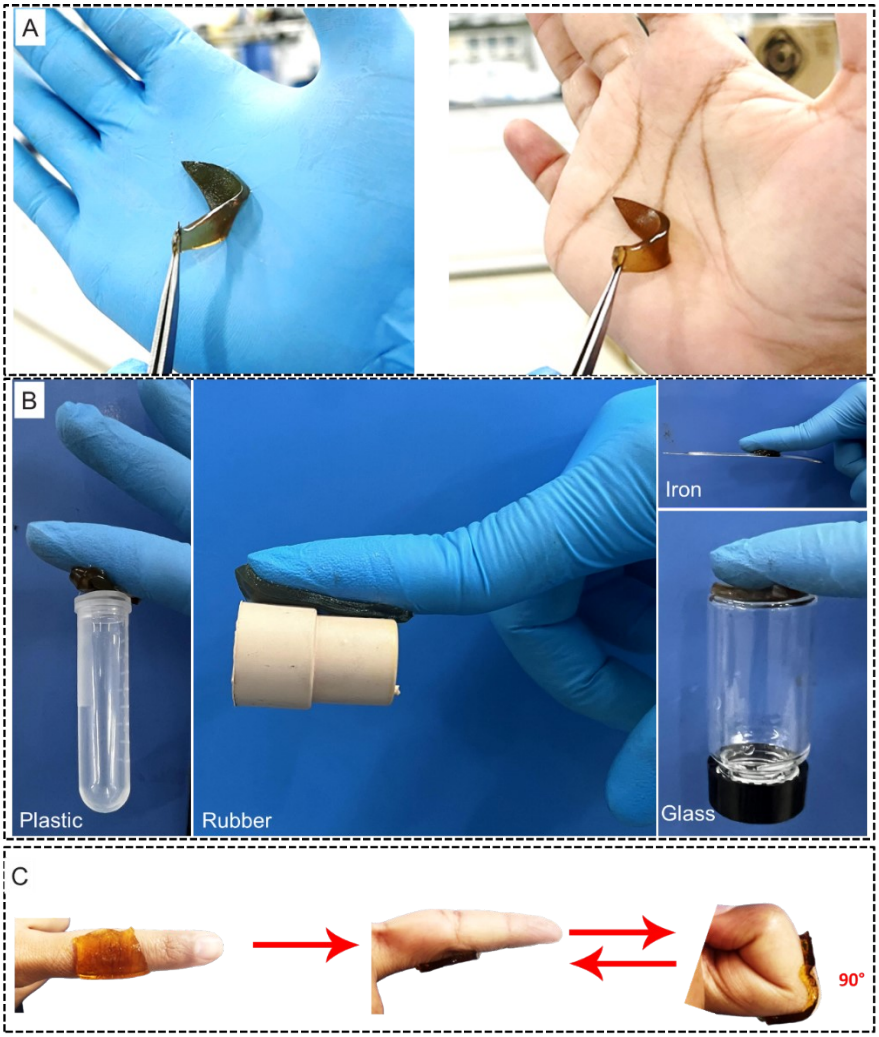

Fig. S6 (A) Hydrogels adhered to hands both with and without glove which can be peeled off without leaving any residue. (B) Hydrogels adhered to various organic and inorganic surfaces. (C) Adhesive behavior of PAM/Ag@HA hydrogel on finger joint.

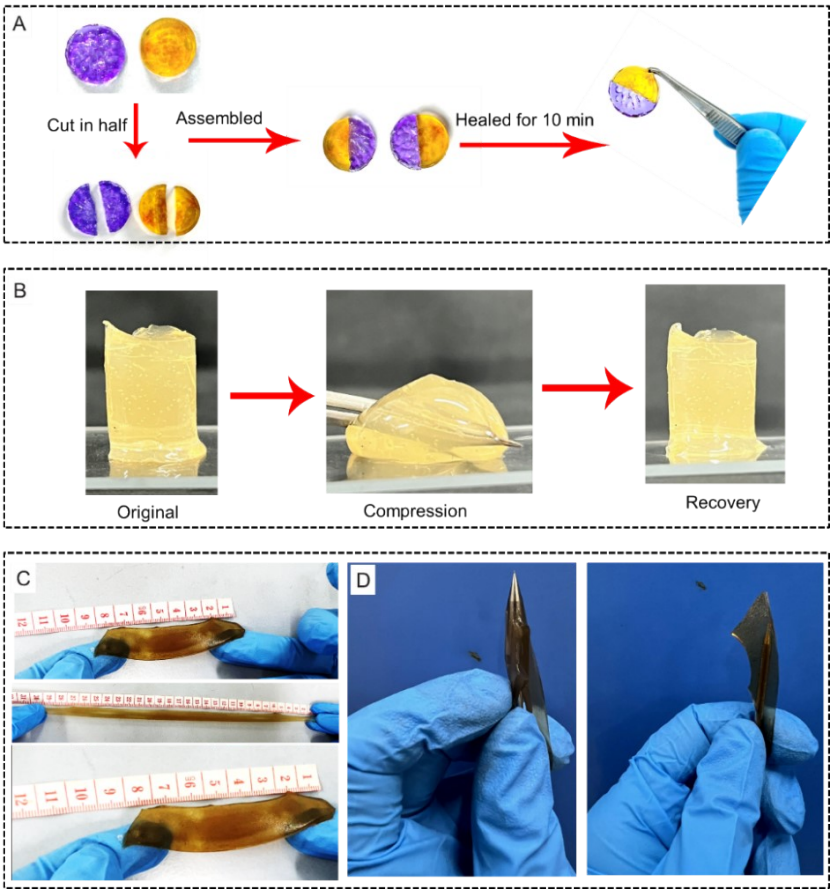

Fig. S7 Macroscopic self-healing behavior of PAM/Ag@HA hydrogel: (A) Two disk-shaped hydrogels (one dyed for visual contrast) were cut in half and reassembled. The segments rapidly self-healed into a single, continuous block at room temperature without the need for any external stimuli. (B) Photographs of the hydrogels withstanding compression. (C) Digital photos of the tensile test by stretching PAM/Ag@HA hydrogel. (D) Puncture resistance.

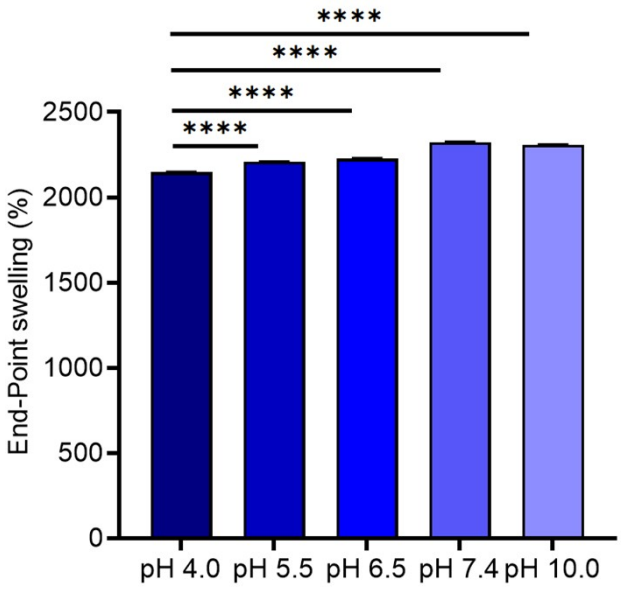

Fig. S8 Endpoint swelling (%) of the hydrogel after 24 h. (n = 3, mean ± SD; ****p < 0.0001)

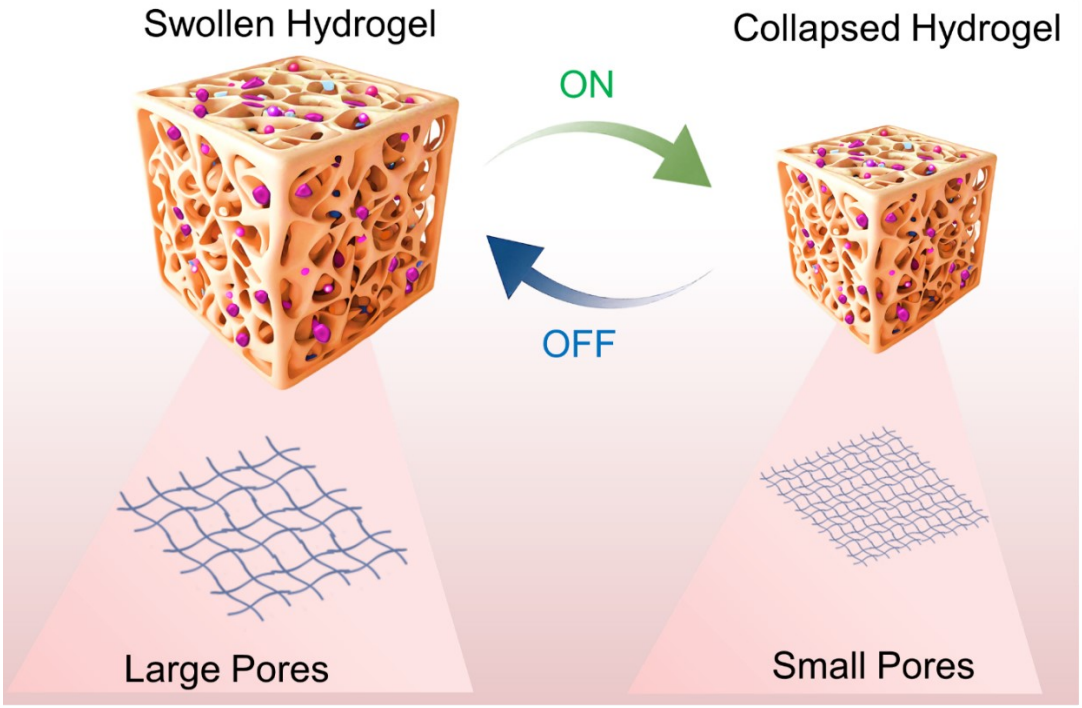

Fig. S9 Schematic illustration depicting the pH-responsive phase transition of the hydrogel, showing the transition from an expanded/swollen state to a contracted/collapsed state.

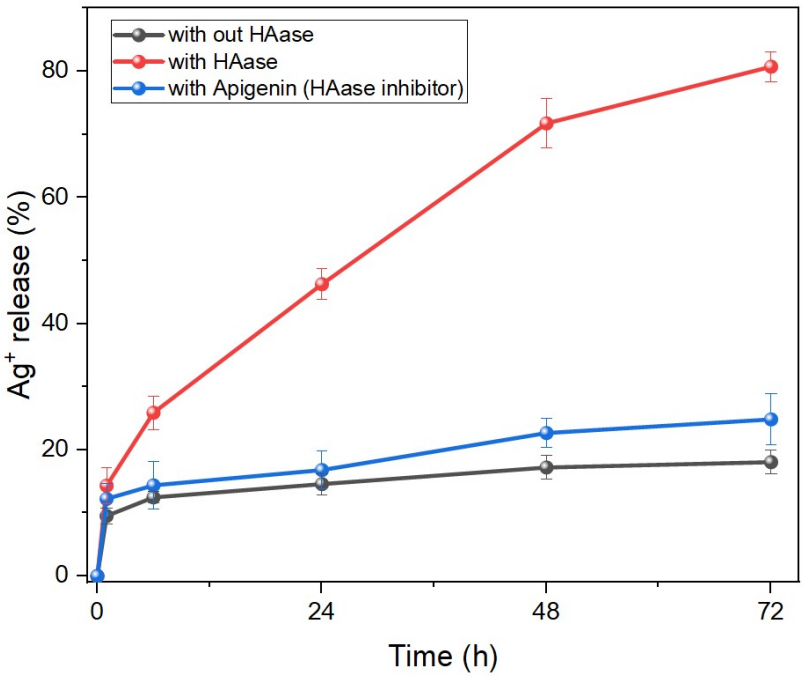

Fig. S10 Release behavior of Ag^+ induced by hyaluronidase (HAase). Release percentage of Ag^+ from PAM/Ag@HA hydrogel under different conditions: in the absence of HAase, in the presence of HAase (100 U mL^{-1}), and in the presence of HAase with Apigenin (HAase inhibitor) over 72 h (n = 3).

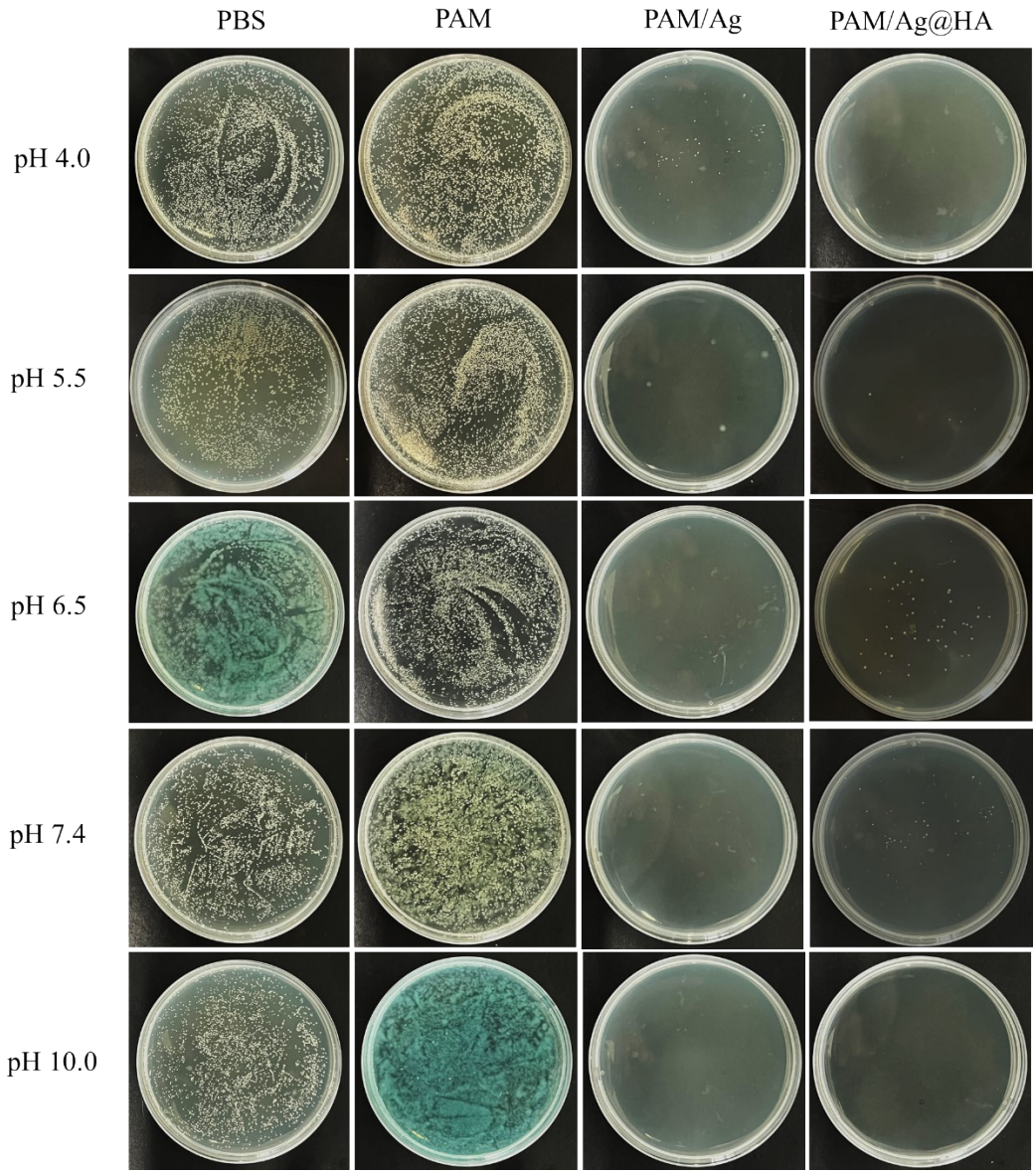

Fig. S11 Photographs of *E. coli* colonies (1×10^6 CFU mL^{-1}) grown on agar plates treated with different hydrogel formulations under varying pH conditions.

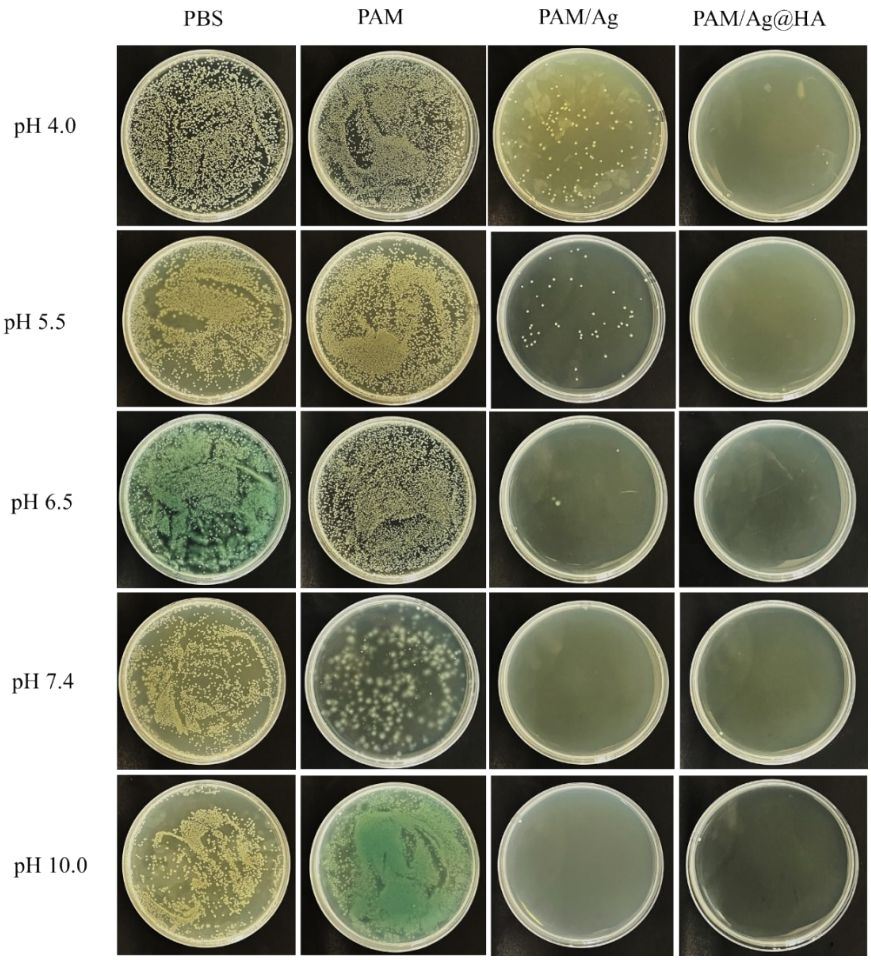

Fig. S12 Photographs of *S. aureus* colonies (1×10^6 CFU mL^{-1}) grown on agar plates treated with different hydrogel formulations under varying pH conditions.

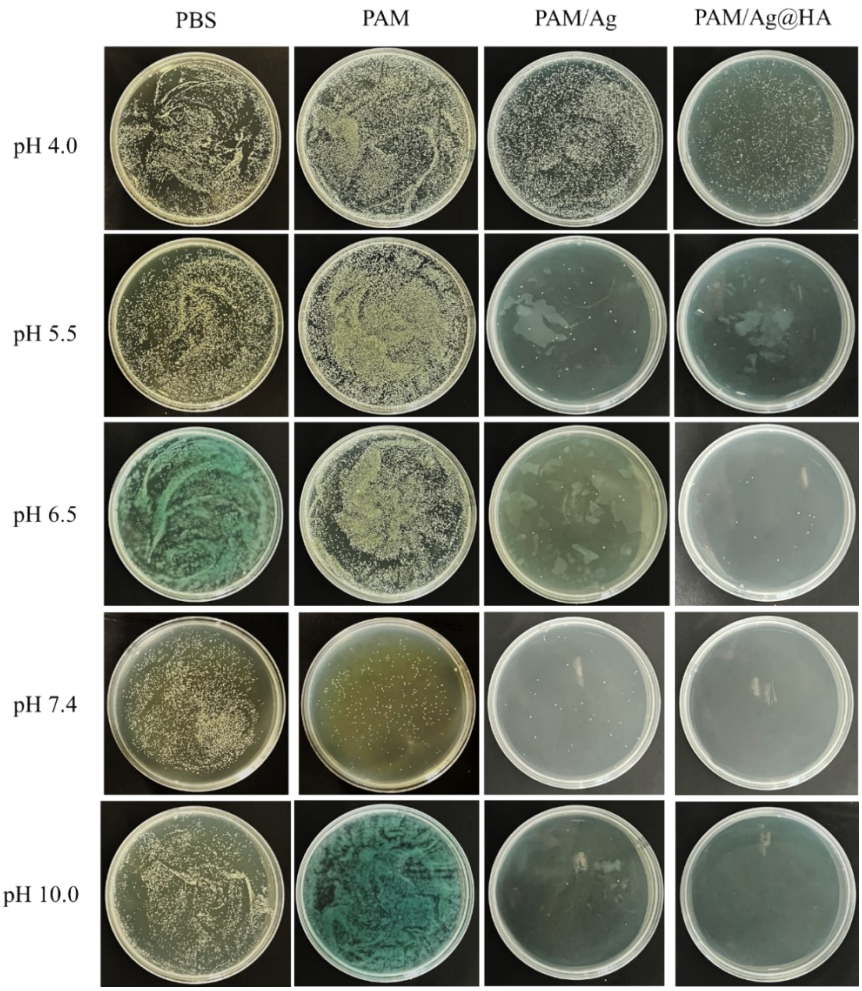

Fig. S13 Photographs of MRSA colonies (1×10^6 CFU mL^{-1}) grown on agar plates treated with different hydrogel formulations under varying pH conditions.

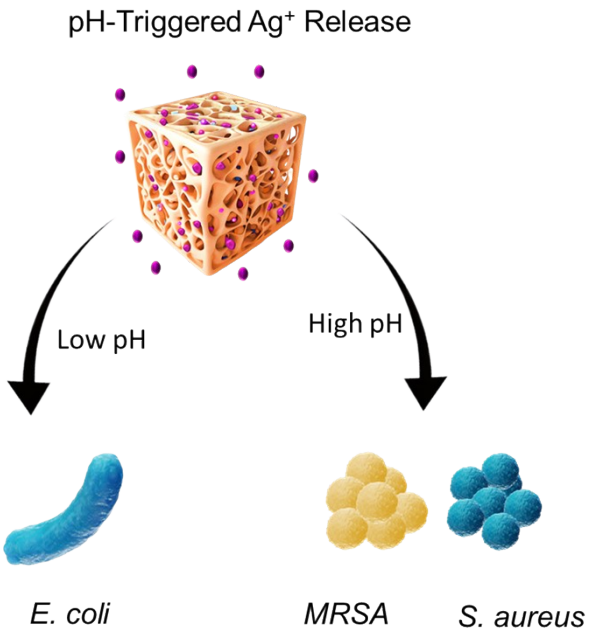

Fig. S14 Smart antibacterial behavior of PAM/Ag@HA hydrogel under varying pH conditions.

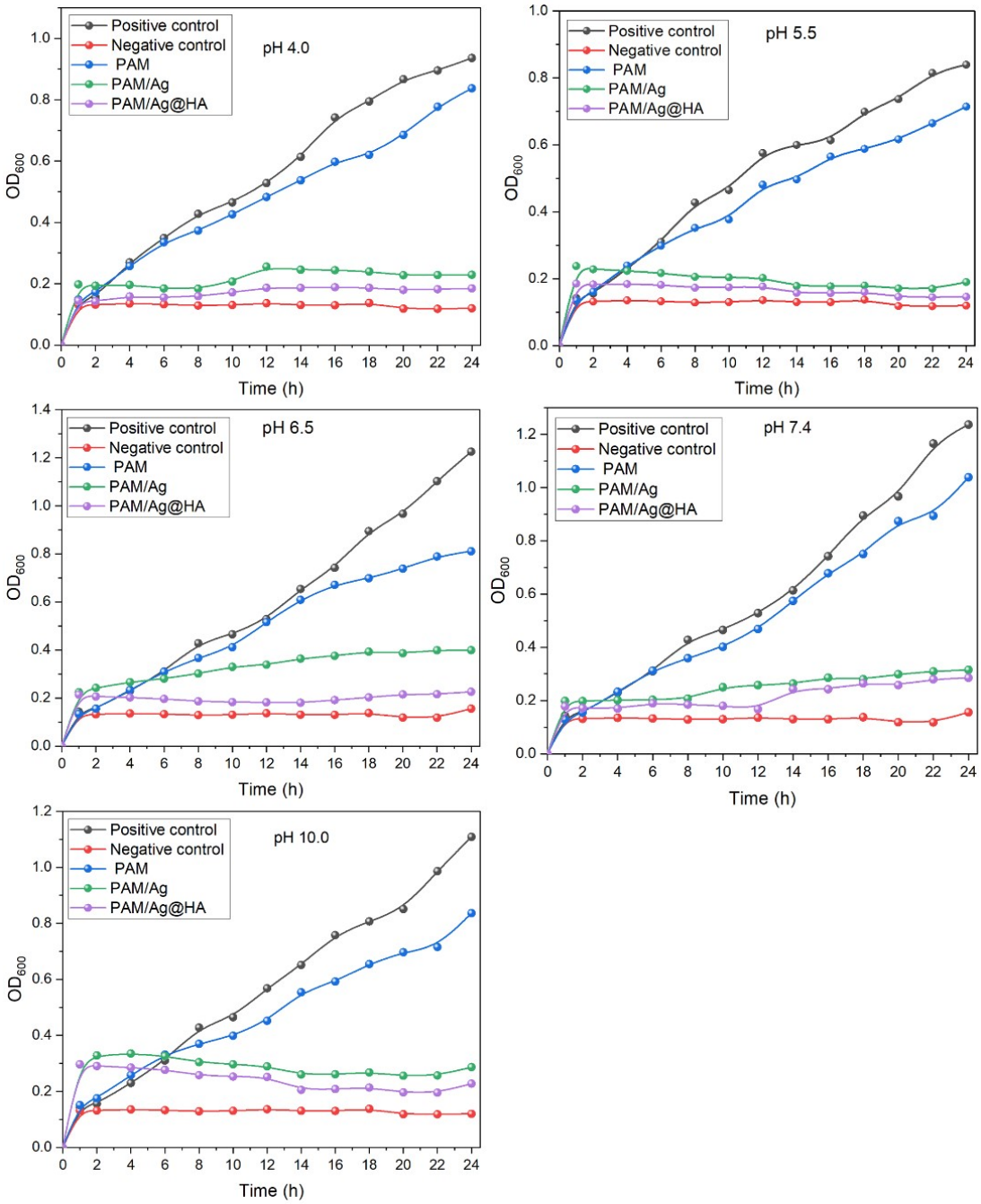

Fig. S15 Growth kinetics of *E. coli* incubated with different types of hydrogels under varying pH conditions.

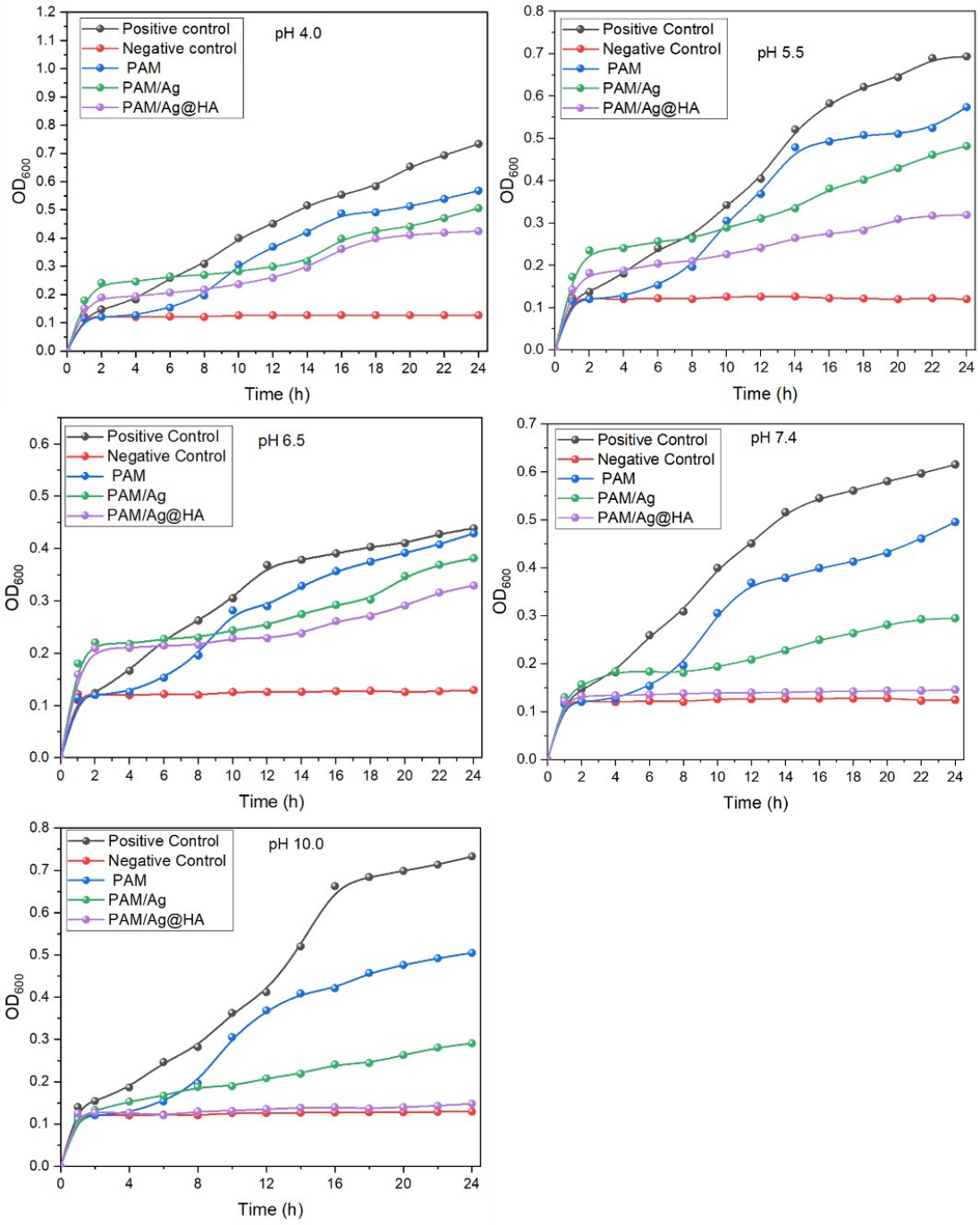

Fig. S16 Growth kinetics of *S. aureus* incubated with different types of hydrogels under varying pH conditions.

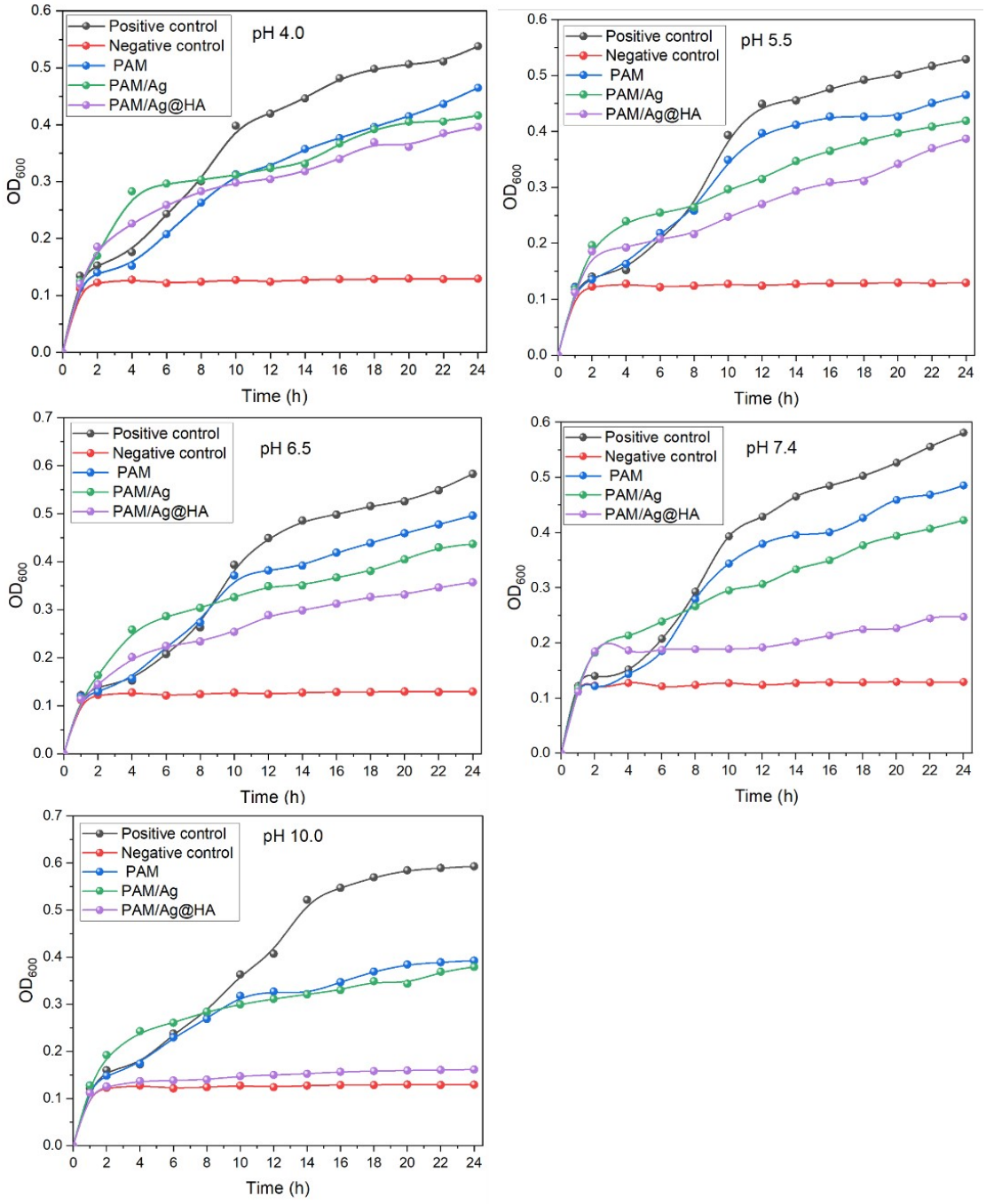

Fig. S17 Growth kinetics of MRSA incubated with different types of hydrogels under varying pH conditions.

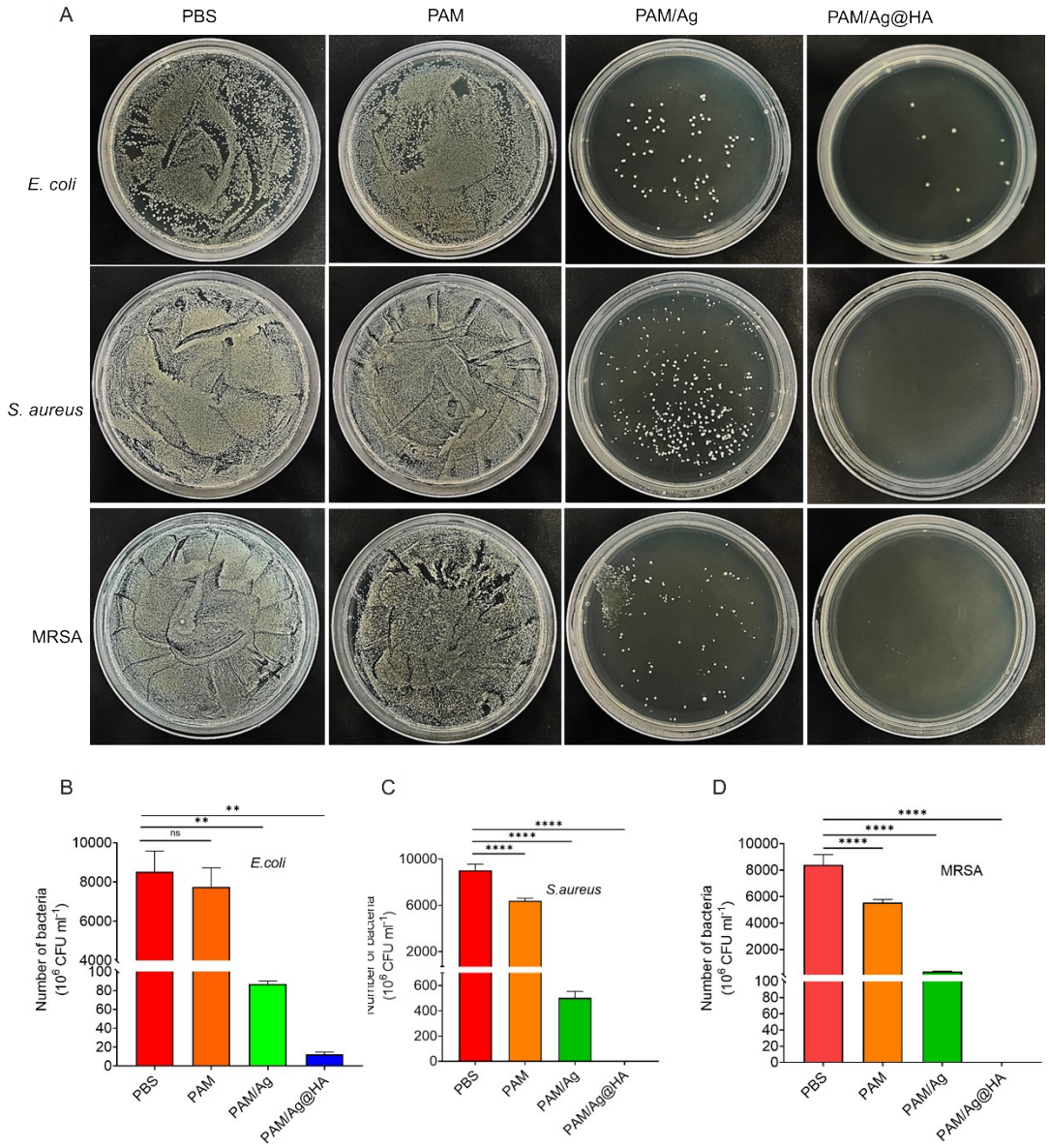

Fig. S18 (A) Photographs of agar plates and accompanying statistical data after 24-h coculture with different hydrogels (1×10^6 CFU mL^{-1}): (A, B) *E. coli*, (A, C) *S. aureus* and (A, D) MRSA. (n = 3, mean ± SD) (**p < 0.01 and ****p < 0.0001; ns, not significant).

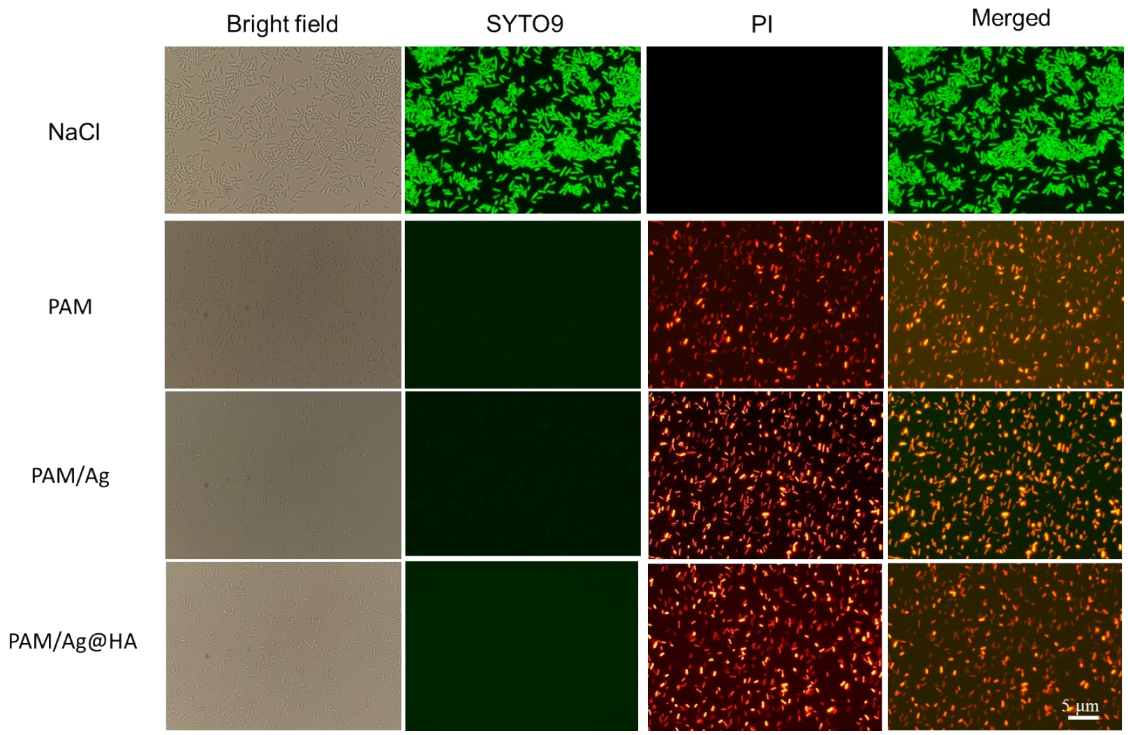

Fig. S19 Live/dead staining experiments of *E. coli* treated with various hydrogels at 16 mg mL^{-1} (scale bar is 5 μm).

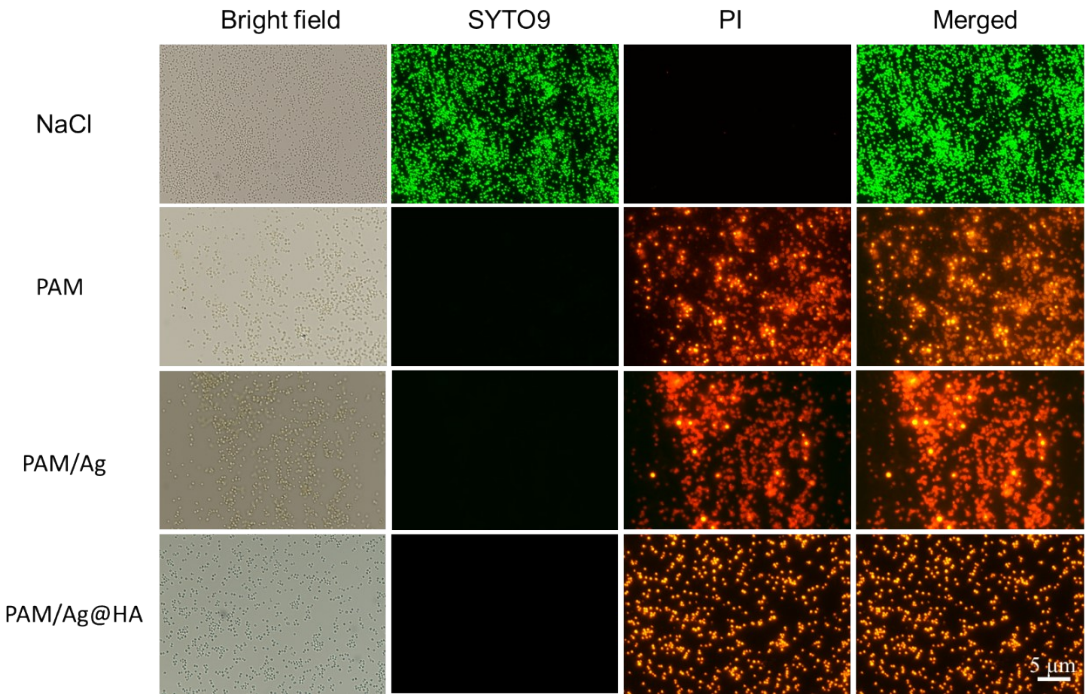

Fig. S20 Live/dead staining experiments of *S. aureus* treated with various hydrogels at 16 mg mL^{-1} (scale bar is 5 μm).

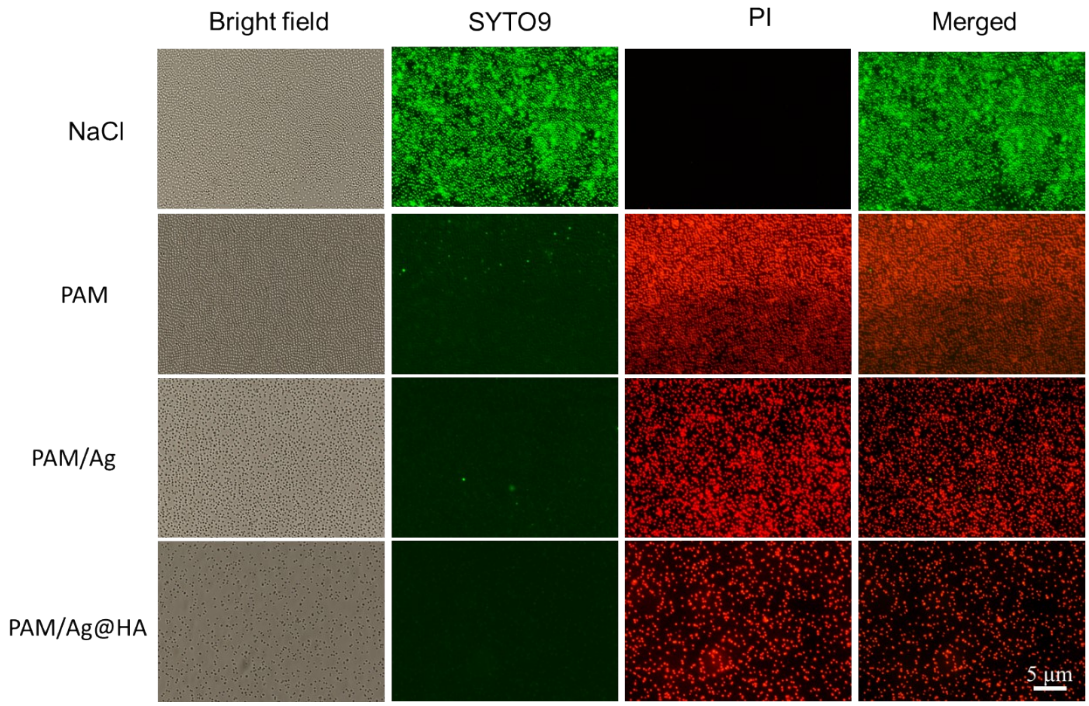

Fig. S21 Live/dead staining experiments of MRSA treated with various hydrogels at 16 mg mL^{-1} (scale bar is 5 μm).

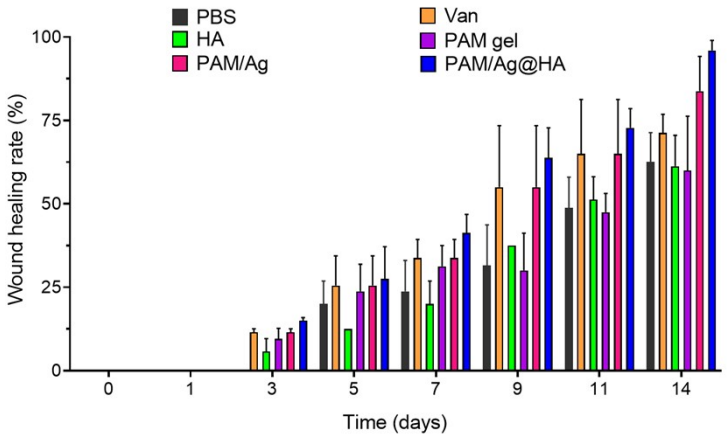

Fig. S22 Quantitative analysis of wound healing rates over 14 days (n = 5).

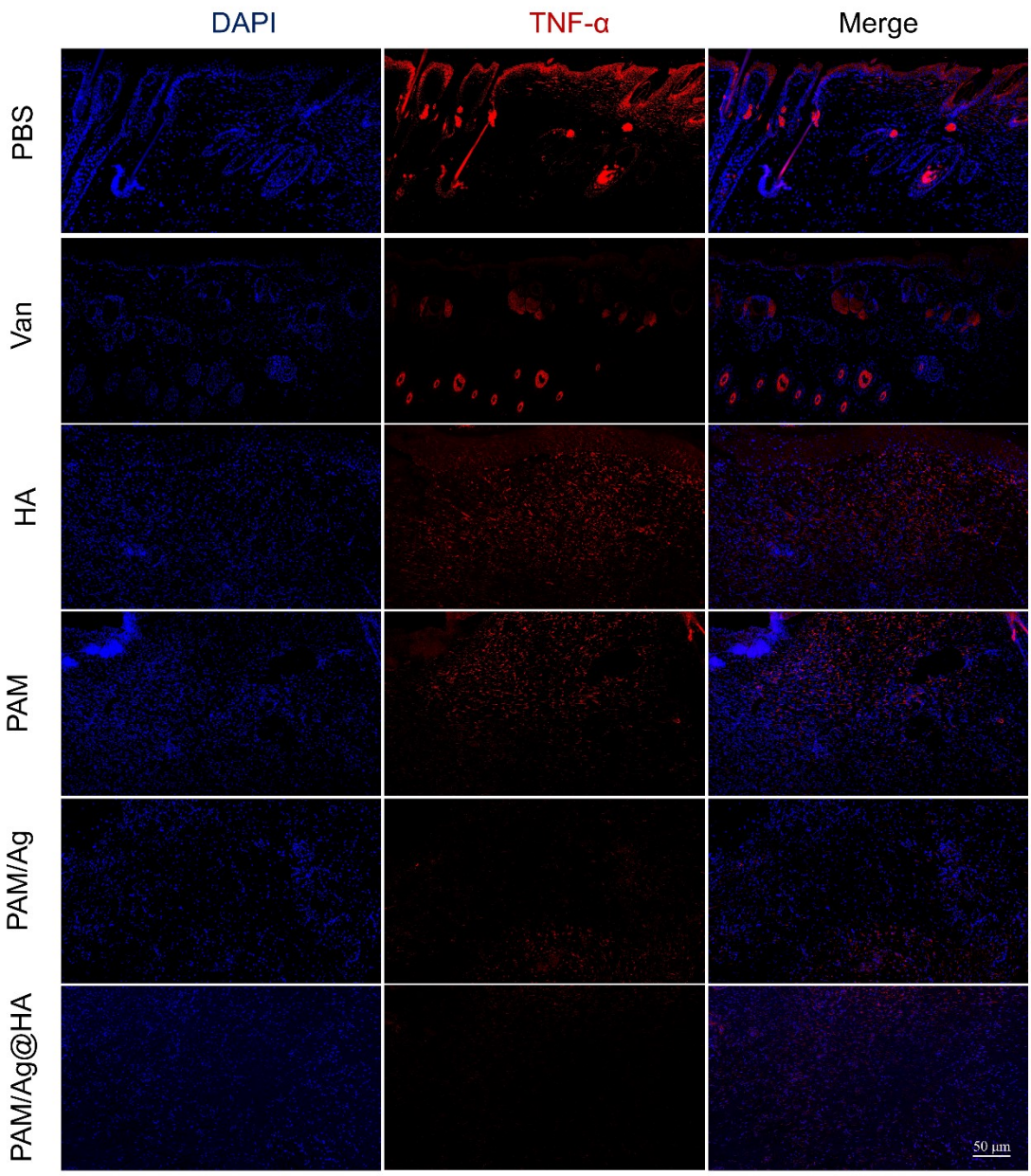

Fig. 23 Immunofluorescence images of TNF-α after different treatments. Scale bar = 50 μm.

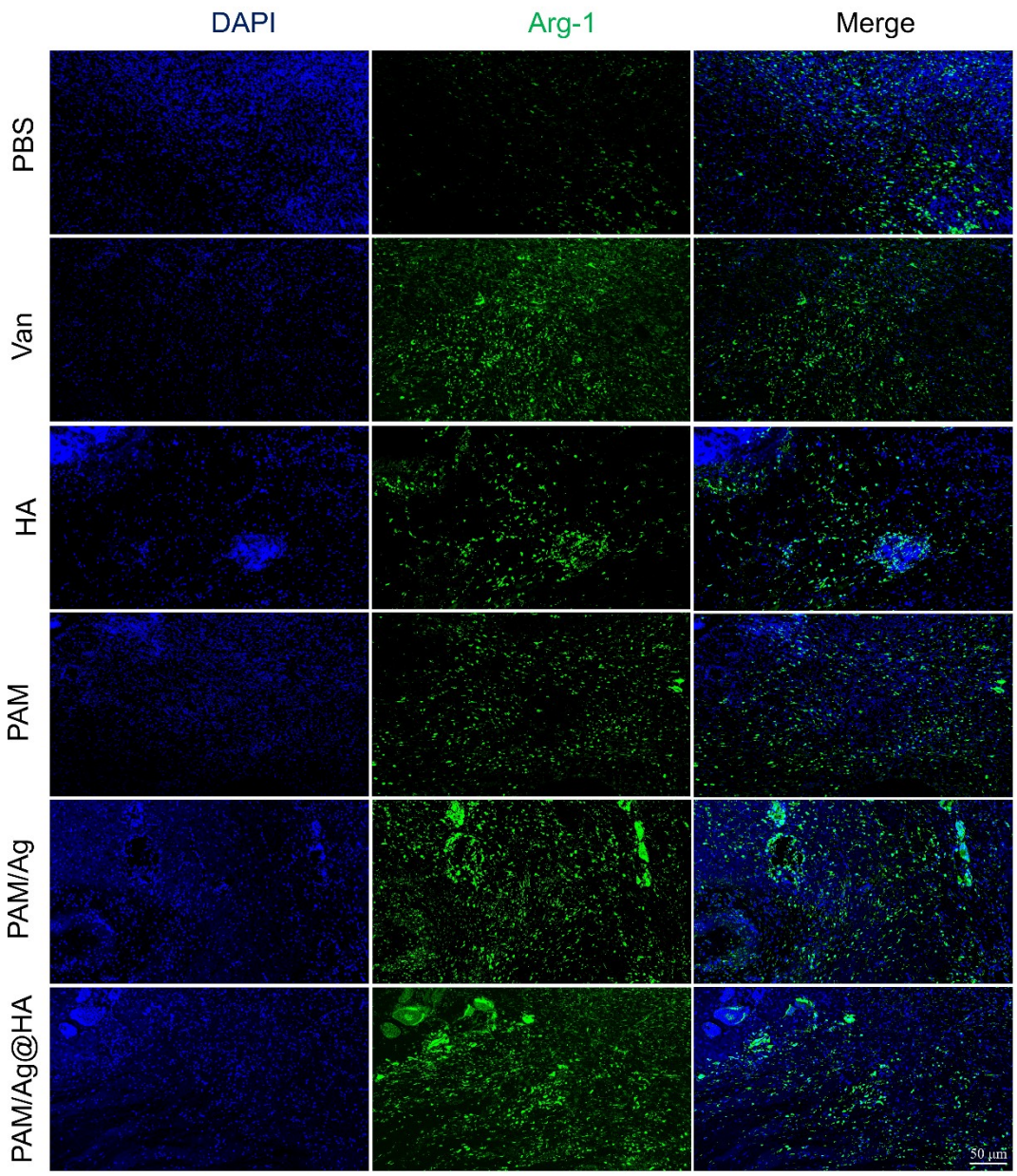

Fig. S24 Immunofluorescence images of Arg-1 after different treatments. Scale bar = 50 μm.

References

1. A. Rasool, S. Ata and A. Islam, *Carbohydr. Polym.*, 2019, **203**, 423-429.
2. Y. Zhong, X. Qin, Y. Wang, K. Qu, L. Luo, K. Zhang, B. Liu, E. A. M. S. Obaid, W. Wu and G. Wang, *ACS Appl. Mater. Interfaces.*, 2021, **13**, 33862-33873.
3. H. Haidari, R. Bright, Z. Kopecki, P. S. Zilm, S. Garg, A. J. Cowin, K. Vasilev and N. Goswami, *ACS Appl. Mater. Interfaces.*, 2022, **14**, 390-403.
4. X. Wang, J. Huang, J. Zhao, T. Yue, W. Shenyang, Y. Xu, Y. Lu and Y. Zhou, *International Journal of Biological Macromolecules*, 2025, **292**, 139201.
5. L. Bonetti, A. Fiorati, A. D'Agostino, C. M. Pelacani, R. Chiesa, S. Farè and L. De Nardo, 2022, **8**, 298.
6. H. Haidari, Z. Kopecki, A. T. Sutton, S. Garg, A. J. Cowin and K. Vasilev, *Antibiotics (Basel, Switzerland)*, 2021, **10**.
7. H. Haidari, K. Vasilev, A. J. Cowin and Z. Kopecki, *ACS Applied Materials & Interfaces*, 2022, **14**, 51744-51762.
8. J. Chen, X. Zhao, L. Qiao, Y. Huang, Y. Yang, D. Chu and B. Guo, *Adv Healthc Mater*, 2024, **13**, e2303157.